CD14 deficiency alters osteoclastogenesis and subchondral bone remodeling after joint injury in mice

Lance A. Murphy[1,2], Kevin G. Burt[1,2], Baofeng Hu[1,2], Vu Nguyen[1,2], Robert L. Mauck[1,2], Carla R. Scanzello[1,2]
[1]University of Pennsylvania, Perelman School of Medicine, Philadelphia, PA;
[2]CMC VA Medical Center, Translational Musculoskeletal Research Center, Philadelphia, PA
Disclosures: LAM (N) - Lance.murphy@pennmedicine.upenn.edu, BH (N), KGB (N), MW (N), VN (N), RLM (4, 5, 8), CRS (8)

INTRODUCTION: Osteoarthritis (OA) not only impacts cartilage within the joint, but it is also associated with bone changes such as subchondral sclerosis and osteophyte formation (1). Toll-like receptor (TLR) ligands have been implicated in the severity and progression of OA after tissue injury and with degeneration (2). CD14 is a GPI-anchored surface protein that is a co-receptor for several TLRs and is highly expressed in myeloid cell lineages, including the precursors of osteoclasts (OCs) (3,4). Notably, our group previously showed that CD14-deficient mice have less subchondral bone remodeling after joint injury (in a DMM (destabilization of the medical meniscus)-model of OA) (5). To understand the cellular activities underlying the differential bone remodeling observed after joint injury with CD14 deletion, we investigated how CD14-deficient OCs form *in vivo* and *in vitro*. ***We hypothesized that depletion of CD14 would protect against TLR4-dependent inhibition of osteoclastogenesis.***

METHODS: Destabilization of the medial meniscus (DMM): DMM or sham surgery (n=5 per group) was performed on male C57BL/6 (WT) and CD14$^{-/-}$ mice at 10-12 weeks of age. Histology (n=4-5 per group): Knees were harvested at 4 weeks post-DMM, then fixed, decalcified, and paraffin embedded. Tissue sections were stained with the Leukocyte Acid Phosphatase kit (Sigma-Aldrich). Focusing on the medial tibial plateau, cell number and trabecular surface area covered by OCs was measured across five 40X fields per mouse, and normalized by total trabecular surface area (ImageJ). Cell isolation and culture: For *in vitro* studies, bone marrow (BM) was pooled from the femora and tibiae of 3 mice for each strain (WT and CD14 knockout) mice. Cells were cultured in complete αMEM + 30 ng/mL M-CSF for 5 days to expand OC precursors. Cells were then replated and cultured with RANKL (100 ng/mL) to induce osteoclastogenesis over 4 days. LPS (1 ng/mL, to activate CD14/TLR4 signaling) and a small molecule TLR4 inhibitor (CLI-095), were added alone or in combination to some cultures. TRAP (tartrate-resistant acid phosphatase) staining and image analysis: Cells were stained for TRAP 3 or 4 days after addition of RANKL. Cells were imaged under 10X brightfield (5 images/well with 4 wells/timepoint), and OCs were identified by their TRAP staining and multinucleation. Images were quantified for percent area of the field covered with OCs (CellProfiler). Flow Cytometry (n=5-6): Freshly isolated BM cells, as well as BM cells that had been expanded for 5 days in M-CSF were analyzed by flow cytometry after staining for cell viability, and mAbs directed against CD45, CSF1R (CD115), and RANK. To quantify differences in bone marrow myeloid progenitor populations (common myeloid, megakaryocyte-erythroid, and granulocyte-macrophage progenitors), freshly isolated bone marrow was stained with a lineage cocktail for terminally differentiated cells, as well as mAbs directed against c-Kit, Sca1, CD34, CD150, and CSF1R and analyzed by flow cytometry. Statistics: Unpaired t-tests were used to test differences between groups. Holm-Sidak correction was employed when multiple t-tests were used.

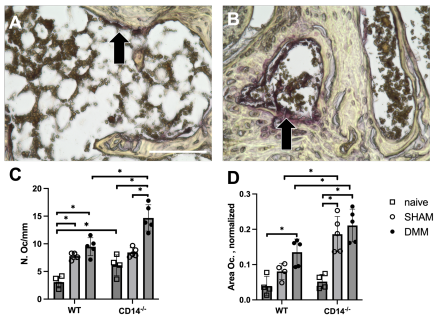

Figure 1: Representative pictures of TRAP staining in WT (**A**) and CD14-deficient (**B**) murine medial tibial plateaus 4 weeks post-DMM. Quantification of cell number (**C**) and trabecular surface covered by TRAP+ cells (**D**) normalized by trabecular surface area. *p<.05, scale bar = 100 µm.

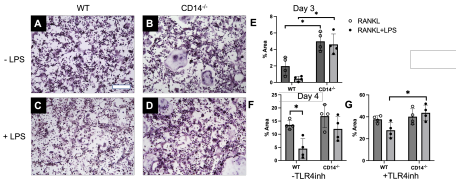

Figure 2: Representative images after 4 days of RANKL exposure of WT OC cultures without LPS (**A**) and with LPS (**C**) and CD14$^{-/-}$ OC cultures without LPS (**B**) and with LPS (**D**). Cell area on day 3 after RANKL with and without LPS (**E**). Quantification of OC percent area on day 4 without TLR inhibition (**F**) and with TLR inhibition (**G**). *p<.05, scale bar = 100 µm.

RESULTS: Representative TRAP staining in WT (**Fig 1A**) and CD14$^{-/-}$ medial tibial plateaus (**Fig 1B**) are shown. OC number and trabecular area covered by OC increased in both strains after both sham and DMM surgeries (**Fig 1 C,D**), but were higher in both naïve and injured knees from CD14-deficient mice, indicating that OC presence increases both with injury as well as with CD14-deficiency *in vivo*. For our *in vitro* experiments, after 3 days of RANKL treatment, cells from CD14-deficient mice showed more osteoclastic differentiation than WT cells, both in the absence and in the presence of LPS (**Fig 2 E**). By day 4, WT and CD14-deficient OCs showed similar area coverage in the absence of LPS (**Fig 2F**). However when LPS was added, WT osteoclastogenesis decreased significantly by 67%, whereas CD14-deficient osteoclastogenesis decreased only by 29% and was not significant. In the presence of CLI-095, WT osteoclastogenesis decreased with the addition of LPS, whereas CD14-deficient osteoclastogenesis did not (**Fig 2 F,G**). Evaluating differences after expansion, flow cytometric analysis of culture expanded (but nondifferentiated) precursors revealed a slight increase in CSF1R positivity in CD14-deficient cells and freshly isolated bone marrow (**Fig 3A**). Interestingly, CD14-deficient precursors had less RANK positivity (**Fig 3A**). However, no difference in abundance of progenitor populations from freshly isolated BM was observed (data not shown). Within the myeloid progenitors, we found no difference in CSF1R (**Fig 3B**).

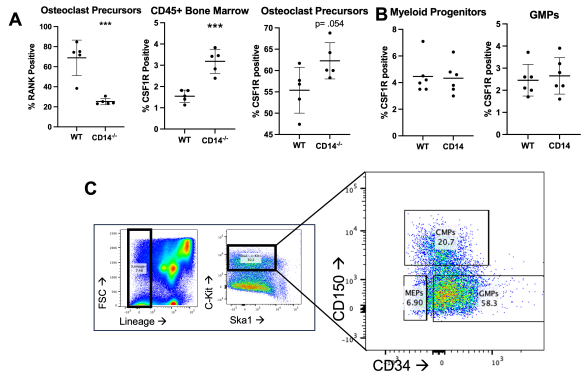

Figure 3: Percent positivity of CSF1R in osteoclast precursor expanded population, percent positivity of RANK in osteoclast precursor expanded population, percent positivity of CSF1R in bone marrow (A). Percent positivity of CSF1R in myeloid progenitor populations (B). Flow schematic for isolating myeloid progenitor populations (C). CMPs: Common myeloid progenitors, MEPs: megakaryocyte-erythroid progenitor, GMPs: granulocyte macrophage progenitor. *** p<.001

DISCUSSION: Our results show that CD14-deficient mice possess an increased presence of OCs in the medial tibial plateau both at baseline and 4 weeks after DMM or sham injury. Additionally, *in vitro,* CD14-deficient OC precursors differentiate into OCs faster than WT controls in response to RANKL, and were less sensitive to the effects of LPS. It has been shown that TLRs 1-9 are present in OC precursors and the activation of TLRs can decrease osteoclastogenesis (6). Analysis of bone marrow populations did not reveal differences in proportions of myeloid progenitor cells between strains, but did reveal a higher expression of CSF1R on OC precursors both at baseline (freshly isolated) and after exposure to M-CSF which may contribute to faster differentiation into OC. However, the decrease in RANK positivity on precursors was unexpected, and suggests that CD14 deficiency is modulating OC inhibitory pathways or activating RANK-independent mechanisms which can be explored in future work. Future work will explore the precise mechanism by which this occurs.

SIGNIFICANCE/CLINICAL RELEVANCE: It is possible that the protection from subchondral bone thickening observed in the DMM model (5) is due to the increased presence of OCs seen in the CD14 deficient mice. Understanding the role of CD14/TLR signaling in osteoclastogenesis may lead to new therapeutic strategies for diseases characterized by pathologic bone remodeling.

REFERENCES: [1] Donell, S *EFORT* 2019; [2] Miller, R+ 2019 [3] Zanoni, I+ *Front Cell Infect. Microbiol.* 2013; [4] Xue, J+ *Art Res Ther* 2020; [5] Sambamurthy, N+ *PLoS ONE 2018*; [6] Ding P+ *Bone Res* 2022